Eur. Phys. J. D **14**, 89–95 (2001)

THE EUROPEAN PHYSICAL JOURNAL D

EDP Sciences

Binding energies of first and second shell water molecules in the $Fe(H_2O)_2^+$, $Co(H_2O)_2^+$ and $Au(H_2O)_2^+$ cluster ions

L. Poisson, P. Pradel, F. Lepetit, F. Réau, J.-M. Mestdagh[a], and J.-P. Visticot

Laboratoire Francis Perrin[b], CEA/DRECAM/Service des Photons, Atomes et Molécules C.E. Saclay, 91191 Gif-sur-Yvette Cedex, France

Received 22 September 2000 and Received in final form 08 December 2000

Abstract. The fragmentation cross-section of the $Fe(H_2O)_{1,2}^+$, $Co(H_2O)_{1,2}^+$ and $Au(H_2O)_{1,2}^+$ ions were measured, as a function of the collision energy. Threshold energies of 1.4 ± 0.2 eV, 1.4 ± 0.2 eV and 1.7 ± 0.1 eV were measured for the monohydrated Fe^+, Co^+ and Au^+ ions respectively, in fair agreement with the existing literature. Small threshold energies of 0.7 ± 0.2 eV, 0.7 ± 0.2 eV and 0.5 ± 0.1 eV were found for the $Fe(H_2O)_2^+$, $Co(H_2O)_2^+$ and $Au(H_2O)_2^+$ clusters respectively. Secondary thresholds were observed on the cross-section, respectively at 1.7 ± 0.3 eV and 2.0 ± 0.2 eV for the $Co(H_2O)_2^+$ and $Au(H_2O)_2^+$ clusters. This double threshold behavior could be attributed to the presence of two kinds of isomers in the beam. The upper threshold is associated with clusters where both water molecules are linked to the metal ion (first solvation shell), whereas the lower threshold corresponds to clusters with one water molecule in the first solvation shell and the other in the second shell. Such an analysis documents the binding energy of either a first shell or a second shell water molecule in the $M(H_2O)_2^+$ cluster ions.

PACS. 36.40.Mr Spectroscopy and geometrical structure of clusters – 36.40.Qv Stability and fragmentation of clusters

1 Introduction

Since the early works of Magnera *et al.* and Marinelli *et al.* [1,2], the energetics of the solvation of transition metal cations by water molecules has attracted a lot of attention, both in experimental [3,4] and theoretical [5–9] works. Most of this activity has been focused on solvation by a few water molecules, located in the first solvation shell, *i.e.* directly attached to the metal ion. This conformation corresponds to the most stable ions, at least when the number of water molecules attached to the metal is not too large [5]. Nevertheless, the possibility of a water molecule in the second solvation shell of a transition metal ion has been considered theoretically by Bauschlicher and collaborators as an excited conformation of the $Cu(H_2O)_{3,4}^+$ cluster ions [7].

Solvation of non transition metal ions by water molecules have also been investigated [10]. Several theoretical studies dealing with solvation by more than one water molecule have systematically documented the question whether one or several water molecules are beyond the first solvation shell and build an H-bonded filament structure. For example, the structure of lowest energy of $Mg(H_2O)_3^+$ [11] and $Ca(H_2O)_3^+$ [12] corresponds to the three water molecules in the first solvation shell. In contrast, the structure of lowest energy calculated for $Al(H_2O)_3^+$ corresponds to the $Al(H_2O)_2(H_2O)^+$ structure where two water molecules are in the first solvation shell, and the third one is in the second shell and forms an H-bonded water filament. Moreover, a filament structure is predicted for $Al(H_2O)_2^+$, with an excess energy of only $+0.092$ eV above the most stable structure where both water molecules are in the first solvation shell [10].

Binding energies of molecules in outer solvation shells have been documented qualitatively in a slightly different context: a photofragmentation study of the $Mg(CO_2)_7^+$ clusters [13]. Complex structures where several water molecules solvating the metal ion build a network of hydrogen bonded molecules have also been observed for $Cs(H_2O)_{n>3}^+$ clusters [14].

The present work aims at investigating experimentally the energetics of the $M(H_2O)_{1,2}^+$ (M = Fe, Co and Au) cluster ions. Collision Induced Dissociation (CID) experiment are performed for this purpose, using helium as collision partner. This provides us with information on the binding energy of the water molecules in the $M(H_2O)_{1,2}^+$ ions. The measurements on the monohydrated clusters serve us to calibrate the reliability of the energy measurements. The true purpose of the work is to document the $M(H_2O)_2^+$ clusters. In particular we aim to stabilize clusters where one of the water molecules is in the second solvation shell. These are thermodynamically unstable species which need to be generated in an *out-of-equilibrium* process. The laser ablation technique coupled to a supersonic expansion is used for this purpose.

[a] e-mail: jmm@drecam.saclay.cea.fr
[b] CNRS FRE 2298

Besides the above purpose of documenting the binding energy of second shell water molecules, measuring the energetics of the $Au(H_2O)^+_{1,2}$ clusters is interesting in its own. The binding energies of both $Au(H_2O)^+$ and $Au(H_2O)^+_2$ have been calculated theoretically [15,16], but experimental information is available for $Au(H_2O)^+$ only [17,18].

2 Experimental

Apparatus

A cluster beam is produced in a Smalley source where a vaporization laser is focused on a metal rod (Fe, Co or Au). A pulsed valve is used to generate the beam from a supersonic expansion. The expanding gas contains helium (the carrier gas), water (seeded into helium), plus neutral atoms and positively charged ions coming from the metal rod which is vaporized. The expansion proceeds through a conical nozzle of 2 mm diameter at the neck. The helium stagnation pressure is 2 bar, and the water partial pressure corresponds to the vapor pressure of liquid water at room temperature (*ca.* 10 torr). The resulting beam carries both neutral species and positively charged cluster ions, which need to be extracted and mass selected.

The positively charged species present in the beam, are extracted perpendicularly to the beam, and accelerated up to 470 eV using a Wiley–McLaren device according to a pulsed sequence explained below. An electrostatic gate, located in the field free region following the Wiley–McLaren device allows us to select the desired cluster ions. Their general formula is (Co, Fe or Au)$(H_2O)^+_n$, with $n = 1$, 2 in the present work. Results on larger clusters, up to $n = 10$ will be the subject of a forthcoming paper.

After mass selection, the ions are decelerated to an energy that can be chosen between 10 and 200 eV in the laboratory. In order to reduce ion losses, a parabolic variation of the potential is used. It is made from a series of 11 potential plates. The cluster ions then enter into a chamber where they collide helium. The geometry of the collision chamber was carefully chosen so as the interaction length (31 cm) and the collision gas pressure are accurately known. This turns out to be essential for the absolute determination of collision cross-sections. The collision chamber is not operated as an ion trap. Instead, the cluster ions are guided by an RF-octopole field in the collision chamber. They have enough energy in the laboratory to be collided, and fragmented and still exit the collision chamber. The octopole avoids ions losses due to collisions. The typical residence time of the clusters in the collision chamber is 40 μs.

On the chamber exit, the ions are re-accelerated up to 470 eV by a parabolic accelerator which is a mirror copy of the decelerator used in front of the collision chamber. About 50 μs after exiting the collision cell, the ions enter into a reflectron before being detected. The reflectron allows us to distinguish between parent and fragment cluster ions.

Operating conditions of the Wiley–McLaren device

Considering the present purpose of running experiments at low collision energy, the Wiley–McLaren device cannot be used with the conventional extraction/acceleration procedure. This question has been carefully examined in reference [19]. Briefly, it appears that the extraction and acceleration voltages of the Wiley–McLaren device can never be properly adjusted when subsequently, the selected ions are to be decelerated and re-accelerated. The energy dispersion, typically 10 to 20 eV, inherently given to the extracted ions in the conventional Wiley–McLaren use, precludes indeed to have a good mass resolution after the sequence deceleration-collision-re-acceleration. Moreover this energy dispersion, which is kept by the decelerated ions when collided at low energy, precludes reliable energy threshold measurements in CID experiments. Instead, we have shown in reference [19] that a double pulsed extraction followed by the acceleration at 460 eV must be preferred:

(i) the first extraction pulse has a voltage of 520 V and a duration of typically 2 μs (it depends on the mass of the selecting cluster). It allows the positively charged species present in the extraction zone to start being extracted towards the acceleration zone of the Wiley–McLaren, but with not enough time to reach the acceleration region;
(ii) the second pulse, in continuity with the first one has a lower voltage, 466 V. It drives the ions into the acceleration region. With this configuration the energy dispersion of the extracted and accelerated ions is reduced to 2 eV.

Measurements

The fragmentation of the (Fe, Co or Au)$(H_2O)^+_{1,2}$ clusters is induced by collision with helium. For this purpose, the clusters are slowed down to the desired laboratory energy and are collided with helium in the collision cell. The helium pressure is varied between 1×10^{-5} and 1.2×10^{-3} mbar. It is measured using an ion gauge which had been previously calibrated by comparison with an absolute viscosity gauge. The resulting uncertainty on the absolute cross-section scale is ≈30%. The cross-section itself was determined by fitting the decay of the parent clusters as a function of the helium pressure by a single exponential Beer-Lambert law. The fit introduces no further error on the cross-section determination.

As anticipated in the introduction, several isomers of the selected $M(H_2O)^+_n$ cluster are present in the ion beam. The fragmentation cross-section for CID is certainly not the same for the different isomers. The cross-section that is measured, therefore appears at a weighted average of the cross-sections for each isomer: $\sigma = \sum_i n_i \sigma_i$ if n_i is the relative population of isomer i ($\sum_i n_i = 1$). For this reason, the measured cross-section σ should be rather called an apparent cross-section.

Another cause of uncertainty when measuring the apparent cross-section is the reproducibility of laser vaporization source which can change the relative populations

n_i. This has been checked directly by varying the source conditions (fluence of the ablation laser, timing of the pulsed valve, timing of the ion extraction with respect to the gas pulse). Uncertainties due to the lack of reproducibility of the ion source can be estimated to 10% on the apparent fragmentation cross-section.

The full experiment consists in recording the fragmentation cross-sections as a function of the collision energy. All the reported energies below are center of mass energies, which were varied between 0.6 and 6 eV for $Fe(H_2O)_n^+$ and $Co(H_2O)_n^+$ clusters and between 0.3 and 4.5 eV for $Au(H_2O)_n^+$. The uncertainty on the collision energy is less than 0.15 eV for collisions of $Fe(H_2O)_n^+$ and $Co(H_2O)_n^+$, and less than 0.1 eV for $Au(H_2O)_n^+$ because of its heavier mass. It is due essentially to the residual velocity dispersion in the ion beam and also, to a small extent, to the thermal motion of helium in the collision cell.

The results that are reported in the present work correspond to the decay of the parent cluster ions. Of course fragment ion peaks have been recorded also. They correspond to the loss of a single water molecule. Importantly, the shape of these peaks does not exhibit the tail that would exist in the case where fragmentation still proceed in the acceleration zone after the clusters have left the collision cell. We thus consider that most of the clusters that are to be dissociated have time to do so during the time spent in the collision cell.

3 Results

The fragmentation cross-sections of the $Fe(H_2O)_{1,2}^+$, $Co(H_2O)_{1,2}^+$ and $Au(H_2O)_{1,2}^+$ cluster ions are shown in Figure 1 as a function of the collision energy in the center of mass reference frame. The collision partner is helium.

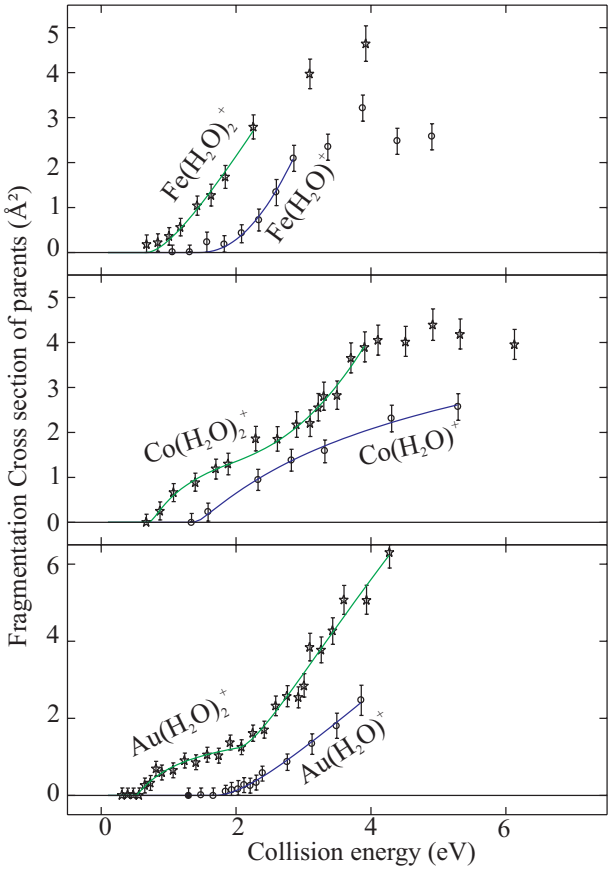

Fig. 1. Apparent fragmentation cross-sections of the $Fe(H_2O)_{1,2}^+$, $Co(H_2O)_{1,2}^+$ and $Au(H_2O)_{1,2}^+$ clusters in collision with helium, as a function of the center of mass collision energy. The curves going through the experimental points are fits, performed using expression (1) and the data given in Table 1. See text for details.

(Fe, Co, Au)$(H_2O)^+$

The three fragmentation cross-sections exhibit a threshold energy followed by a monotonic increase. In order to get an estimate of the threshold energy, the experimental points were fitted using the expression:

$$\sigma(E) = \sigma_0 \frac{(E - E_{\text{Threshold}})^n}{E} \cdot \qquad (1)$$

Such an expression has already been used in references [4,19]. E is the collision energy and $\sigma(E)$ is the measured cross-section. $E_{\text{Threshold}}$, the threshold energy for dissociation, n and σ_0 are three adjustable parameters. The best fit values are given in Table 1. We focus on $E_{\text{Threshold}}$ only. Its accuracy is limited to 0.2 eV for $Fe(H_2O)^+$ and $Co(H_2O)^+$ and to 0.1 eV for $Au(H_2O)^+$, essentially because of the small fragmentation cross-section and the energy dispersion in the ion beam. Considering these uncertainties, it is useless to correct the threshold energies as done in the group of Armentrout to account for both the internal energy of the cluster ions and the dispersion of the collision energy [4]. These corrections are negligible indeed in the present context.

Armentrout and coworkers found respectively 1.70 ± 0.06 eV and 1.36 ± 0.05 eV for the binding energy of the water molecule in $Co(H_2O)^+$ and $Fe(H_2O)^+$. Within the error bars, our results are in agreement with these very accurate determinations.

The threshold energy for the CID of $Au(H_2O)^+$ given in Table 1 (1.7 ± 0.1 eV) must be compared to the evaluation of the Au^+–H_2O binding energy performed by Schwarz and coworker in a work which combines theoretical and experimental data (1.6 ± 0.2 eV) [18]. The agreement between both is good. The present result is also in excellent agreement with a CBS-CCSD(T) calculation by Feller *et al.* which yields 1.74 eV for the Au^+–H_2O binding energy [16].

(Fe, Co, Au)$(H_2O)_2^+$

The cross-sections for $Co(H_2O)_2^+$ and $Au(H_2O)_2^+$ exhibits a double threshold. Therefore, expression (1) has been used to fit the cross-section in two steps. The first one consists in adjusting the low energy range, between 0.5 and 2 eV with a single function $\sigma(E)$, thus providing the first threshold. In the second step, the high energy range

Table 1. Parameters of expression (1) used to fit the energy dependences of the CID cross-sections shown Figure 1. For comparison purposes, the last column gives literature data both for $(Fe, Co, Au)(H_2O)^+$ and for the most stable isomer of $(Fe, Co, Au)(H_2O)_2^+$: (a) [4], (b) [18] and (c) [16].

		Threshold	$E_{\text{Threshold}}$	σ_0 (Å^2 eV^{1-n})	n	Literature
Fe	$Fe(H_2O)^+$		1.4 ± 0.2 eV	2.2 ± 0.1	2.6 ± 0.1	1.36 ± 0.05 eV[(a)]
	$Fe(H_2O)_2^+$	first	0.7 ± 0.2 eV	2.3 ± 0.1	2.0 ± 0.1	
	$Fe(H_2O)_2^+$	second				1.70 ± 0.04 eV[(a)]
Co	$Co(H_2O)^+$		1.4 ± 0.2 eV	2.5 ± 0.1	1.3 ± 0.1	1.70 ± 0.06 eV[(a)]
	$Co(H_2O)_2^+$	first	0.7 ± 0.2 eV	2.1 ± 0.2	1.1 ± 0.2	
	$Co(H_2O)_2^+$	second	1.7 ± 0.3 eV	0.8 ± 0.1	3.0 ± 0.3	1.68 ± 0.07 eV[(a)]
Au	$Au(H_2O)^+$		1.7 ± 0.1 eV	2.3 ± 0.1	1.8 ± 0.1	1.6 ± 0.2 eV[(b)]
						1.74 eV[(c)]
	$Au(H_2O)_2^+$	first	0.5 ± 0.1 eV	1.6 ± 0.1	1.1 ± 0.2	
	$Au(H_2O)_2^+$	second	2.0 ± 0.2 eV	5.6 ± 1.4	1.6 ± 0.2	2.09 eV[(c)]

between 2 and 5.2 eV is fitted using this function plus a second $\sigma(E)$ function, the parameter of which are adjusted. This provides us with the second threshold. Of course, the uncertainties on the second threshold determination are larger than on the first one.

The values found for the second threshold are respectively 1.7 ± 0.3 eV and 2.0 ± 0.2 eV for $Co(H_2O)_2^+$ et $Au(H_2O)_2^+$. These values must be brought together with the binding energies of H_2O–$M(H_2O)^+$ in clusters where both water molecules are in the first solvation shell. Armentrout and coworkers found 1.68 ± 0.07 eV for $Co(H_2O)_2^+$ [4], which is very close to the present second threshold. The only information available yet on $Au(H_2O)_2^+$ clusters is the calculation of Feller *et al.* at the CBS-CCSD(T) level [16]. A value of 2.09 eV is found, which is in very good agreement with the present second threshold.

The experimental section above has anticipated the ion beam is likely to carry several isomers of the selected $M(H_2O)_n^+$ clusters. Reasons why the present Smalley source does so, whereas the ligand exchange source used in the group of Armentrout does not, are examined in the Appendix. The important point here is that the measured cross-section is an average of the cross-sections associated to each isomer. From the close agreement above between the high energy threshold and the literature data on the most stable $(Co, Au)(H_2O)_2^+$ ions, we assign the high energy threshold to isomers where both water molecules are in the first solvation shell. The low energy threshold is therefore assigned to an excited conformation of the $(Co, Au)(H_2O)_2^+$ ions, tentatively those having a water molecule in the second solvation shell. The difference between both energy thresholds is too large (1 eV for Co and 1.5 eV for Au), and the secondary energy threshold is too distinct to simply interpret the lowest threshold as due to vibrationally hot parent clusters. Instead, we anticipate that the low energy threshold documents the binding energy of the outer water molecule in an excited conformation of the cluster, which nevertheless is cold vibrationally, this excited conformation being trapped in a high lying well of the potential energy surface.

One might be surprised that a filament isomer was not found for $Co(H_2O)_2^+$ in our previous work where the cluster ions were generated using the same source as that used here [19]. Neon was used for CID in this former work and the mass ratio between neon and $Co(H_2O)_2^+$ did not allow us to investigate collision energies below 1.8 eV. As a result, the energy threshold of 1.5 ± 0.1 eV found in this work was an extrapolation at lower energies using a fit of the energy dependence of the cross-section. It was therefore out of question to observe a threshold at even smaller energies.

Only one CID energy threshold is apparent for $Fe(H_2O)_2^+$ in Figure 1. It is measured at 0.7 ± 0.2 eV, and thus corresponds to the low energy threshold for $Co(H_2O)_2^+$ and $Au(H_2O)_2^+$, implying that an excited conformation of the cluster is collided here. The reasons for not observing a distinct secondary threshold with iron is not clear. This might be due to the change of electronic structure of the iron ion when switching from a single water molecule attached to iron as in the filament isomer to two water attached to iron in the stable isomer. It has been shown indeed that the electronic configuration of the iron ion changes from (s^1d^6) to (d^7) when the number of ligands attached to the ion passes from 1 to 2 [5].

4 Discussion

The most important result above concerns the existence of isomers of $(Fe, Co, Au)(H_2O)_2^+$ in the cluster beam, which were tentatively assigned to an excited conformation trapped in a high lying well of the potential energy surface. The energy threshold for the CID of these isomers is quite small: 0.7 ± 0.2 eV, 0.7 ± 0.2 eV and 0.5 ± 0.1 eV respectively for the $Fe(H_2O)_2^+$, $Co(H_2O)_2^+$ and $Au(H_2O)_2^+$ cluster. It is likely related to the CID of a filament isomer where one of the water molecule is in the second solvation shell. The value 0.7 ± 0.2 eV, 0.7 ± 0.2 eV and 0.5 ± 0.1 eV thus appear as the binding energy of the second shell water molecule in the $Fe(H_2O)_2^+$, $Co(H_2O)_2^+$ and $Au(H_2O)_2^+$ cluster ions respectively.

Several points concerning the filament isomers will be discussed successively in order to substantiate the above consideration. Firstly, we discuss the existence of a secondary well in the $M(H_2O)_2^+$ potential energy surfaces in the light of a preliminary calculation by Maître on the $Co(H_2O)_2^+$ ion. Secondly, we examine the stability of the filament isomer under the beam conditions. Thirdly, coming back to $Fe(H_2O)_2^+$, $Co(H_2O)_2^+$ and $Au(H_2O)_2^+$, we discuss the binding energy of the outer water molecule in the light of simple electrostatic arguments. Finally, turning to Figure 1 we observed that the CID cross-sections are much smaller than geometrical cross-sections. A model of the He-cluster energy transfer is proposed at the end of the discussion to account for this observation.

A secondary well in the $Co(H_2O)_2^+$ potential energy surface

Maître [20] has provided us with preliminary calculations on the $Co(H_2O)_2^+$ cluster. The calculations were done at the CASPT2 level. They reveal the existence of a filament structure $Co^+(H_2O)(H_2O)$, which is 1 eV more energetic than the most stable structure with the two water molecules in the first shell. This result is strikingly in agreement with the present work since 1 eV is also the energetic distance between the first and the secondary thresholds of the present CID experiment (see Tab. 1). The calculations show also that the transition region between the secondary minimum and the most stable structure is 0.1 eV above the secondary minimum. These results are summarized in Figure 2. It is understandable from the figure that the filament isomer may be trapped in the bottom of the high lying potential well.

Stability of the filament structure of $Co(H_2O)_2^+$ under the beam conditions

Beside the energy and the geometry of the filament isomer, the calculation by Maître provides us with the frequencies of the various vibration modes of the cluster ion. A simple RRKM calculation, including corrections for the zero point energy [21–23] shows that the filament isomer is stable at 300 K, a temperature which is much higher than the expected cluster temperature in the beam (100 K). In fact this result is not very surprising considering that at 300 K, three degrees of freedom of the filament cluster are populated, which corresponds to an internal energy of 0.07 eV, an energy which is substantially smaller than the 0.1 eV of the secondary potential well.

Binding energy of the outer water molecule in the filament isomer of $Fe(H_2O)_2^+$, $Co(H_2O)_2^+$ and $Au(H_2O)_2^+$

The bonding of the second shell water molecule in the filament isomers of $Fe(H_2O)_2^+$, $Co(H_2O)_2^+$ and $Au(H_2O)_2^+$ can be separated into two contributions: the water-water H-bond and the interaction with the M^+ ion. This neglects contributions due to the polarization of both water molecules by the metal ion. Of the two major contributions, only the interaction with the positive ion may

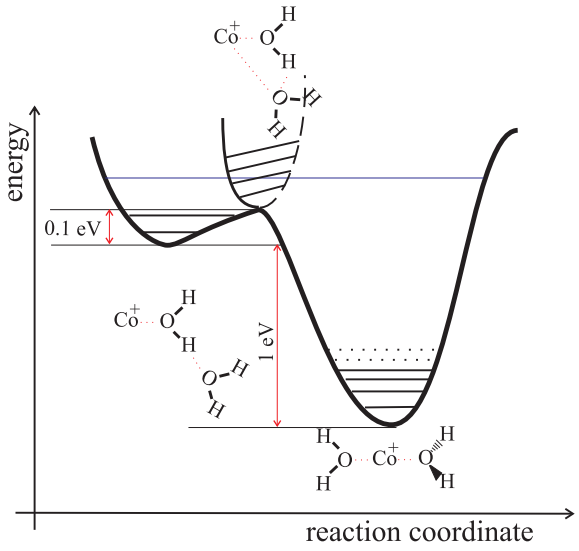

Fig. 2. Scheme showing the likely variation of the potential energy of the $Co(H_2O)_2^+$ cluster ion along an hypothetical reaction coordinate corresponding to the isomerization of the cluster from its most stable structure with the two water molecules in the first solvation shell, to a less stable filament structure. The transition state between both structures is also shown in the figure. The energies at the two minima and that at the transition state were given by a CASPT2 calculation performed by Maître [20]. Note that the structures which appear as planar in the figure are not planar in the calculation.

vary from Fe^+ to Au^+. The size of the metal ion increases indeed from Fe^+ to Au^+. Larger ions maintain the water molecules at larger distances, thus reducing the M^+-*outer water* interaction. This picture is in qualitative agreement with the energy thresholds given in Table 1: the same first threshold of 0.7 eV is measured indeed with Fe^+ and Co^+ which have a comparable size, whereas a lower threshold of 0.5 eV is measured for the larger Au^+ ion. The picture is however too simple and cannot account quantitatively for the 0.2 eV difference between both threshold energies.

Energy transfer mechanism in CID by helium

Let us recall that the measured cross-section $\sigma(E)$ (E is the collision energy) is the average of the CID cross-sections $\sigma_i(E)$ of the individual isomers, weighted by the population n_i of the isomers:

$$\sigma(E) = \sum_{i=1,2} n_i \, \sigma_i(E) \qquad (2)$$

where $i = 1$ refer to the isomer with both water molecules in the *first* solvation shell and $i = 2$ to the filament isomer where one water molecule is in the *second* shell. Let us observe the $Co(H_2O)_2^+$ data in Figure 1 at 4 eV, *i.e.* at an energy well above both thresholds. The contributions of both isomers to the full cross-section is comparable. Each amounts for about 2 Å^2. Considering that the most stable isomer is probably the dominant species present in

the beam, this indicate that the cross-section $\sigma_1(4\text{ eV})$ is quite small. In other words, fragmentation of isomer 1 (the isomer with only first shell water molecules) by helium, is inefficient. In contrast, since the population of isomer 2 (an excited conformation of $Co(H_2O)_2^+$) is expectedly small, the corresponding CID cross-section σ_2 must be significantly larger than σ_1 to lead to the same contribution to the full cross-section. This question is discussed now by modeling the energy transfer between helium and the cluster ion.

Helium is known to poorly transfer its kinetic energy when colliding an heavy target. This appears on the ground of an impulsive energy transfer as developed in simple models such as those of references [24–26]. This appears also in the molecular dynamics calculations of Hase and coworkers [27], and in the experimental work by Armentrout and coworkers [28] when investigating the CID of VO^+ by various rare gases.

Assuming that the collision between helium and $(Fe, Co, Au)(H_2O)_2^+$ is sudden, we can consider that only one of the constituents of the cluster, the metal ion or one of the water molecules, is collided. The collision energy is then transfered to this particular constituent, and it is transfered to the rest of the cluster in a second step. The impulse model suggests that only 50% of the collision energy is transfered in an helium–H_2O collision and less than 10% in an He–Co^+ collision. However, considering the very small size of helium we can also imagine the collision of helium with a single H atom of the water molecule. In that case, almost 65% of the collision energy is transfered. This corresponds to the optimum energy transfer. In terms of cluster fragmentation, the kick to an H-atom is especially efficient when the H-atom is involved in an H-bond. Any motion of the H-atom, in this case, is indeed strongly coupled to the dissociation coordinate and a direct dissociation may occur. In contrast, when the kick to hydrogen occurs on a first shell water molecules of most stable isomer, only the rotation of water about the M^+-O axis is excited. Such motion is weakly coupled to the dissociation coordinate, hence the system has to wait for and RRKM-like process to dissociate. The cross-section σ_1, which is associated to this energy transfer mechanism is likely to be much smaller than the cross-section σ_2 of the other mechanism where the energy is almost directly channeled into the dissociation coordinate. For this reason we consider that CID by helium is a sensitive probe of second shell water molecules, a property that will be exploited systematically in a forthcoming work on larger $(Fe, Co, Au)(H_2O)_n^+$ clusters.

The question of a poor energy transfer from helium to first shell water also appears when considering the monohydrated species. This is especially visible for $Fe(H_2O)^+$ and $Au(H_2O)^+$ in Figure 1 where the CID cross-section increases very slowly above the threshold. Near the threshold the only fragmentation pathway is indeed the RRKM-like process. The impulsive energy transfer to the whole water molecule, kicking it out of the cluster, should appear well above the threshold. It might be the origin of the sharp increase of the fragmentation cross-section above 2 eV.

5 Conclusion

A laser vaporization source, coupled to a supersonic expansion is used to generate $(Fe, Co, Au)(H_2O)_n^+$ cluster ions. A Wiley–McLaren device operating under a double extraction pulse sequence allows us to extract these ions and accelerate them with a small energy dispersion. After the proper deceleration, these ions are collided with helium before being detected. The results reported in this article concern the CID of the $(Fe, Co, Au)(H_2O)_{1,2}^+$ ions. The CID threshold measured for the monohydrated ions essentially served to test the reliability of the experimental apparatus. Nevertheless, the value of 1.7 ± 0.1 eV found for $Au(H_2O)^+$ served also to confirm the value of 1.74 eV calculated recently by Feller and coworker for the Au^+-H_2O binding energy.

The central part of the work concerns the $Fe(H_2O)_2^+$, $Co(H_2O)_2^+$ and $Au(H_2O)_2^+$ ions. It has been possible to generate and to stabilize excited conformation of these ions. The resulting ion beam thus contains both the stable isomer of the $M(H_2O)_2^+$ ions and isomers corresponding to the excited conformation. This was shown by observing the energy dependence of the CID cross-section. Those for $Co(H_2O)_2^+$ and $Au(H_2O)_2^+$ exhibit two thresholds. The upper one is assigned to CID of the stable isomer having both water molecules in the first solvation shell (*i.e.* directly attached to the metal ion). This threshold is in good agreement with the expected binding energy of a water molecule in such isomers. For $Au(H_2O)_2^+$, no other experimental work is available. The threshold energy that is found here, 2.0 ± 0.2 eV, confirms the calculation by Feller. The low energy threshold, respectively 0.7 ± 0.2 eV, 0.7 ± 0.2 eV and 0.5 ± 0.1 eV for $Fe(H_2O)_2^+$, $Co(H_2O)_2^+$ and $Au(H_2O)_2^+$, is assigned to fragmentation of the other isomer. This isomer is discussed to have a filament structure where one of the water molecule is in the second solvation shell, and is bonded to the first one by an H-bond.

The authors acknowledge P. Maître (LCP Orsay) for a very fruitful collaboration and for providing there with yet unpublished calculation results. This work has been supported by the C.E.A. under the grant "Interaction ion métallique molécule".

Appendix: Comparison between ligand exchange and Smalley type sources

The present appendix examines a few reasons why Smalley type sources which couple laser evaporation to supersonic expansion are likely to produce various isomers of the $M(H_2O)_n^+$ clusters, whereas ligand exchange sources of the type used by Armentrout and coworkers do not [4].

Ligand exchange source

The cluster beam source used in reference [4] works along the ligand exchange technique. Water molecules are exchanged collisionally with carbonyl groups in iron carbonyl clusters $Fe(CO)_5^+$.

The exchange chamber operates at low pressure (0.5–1 mbar). The following exchange mechanism can be imagined. In a first step, a carbonyl group is lost collisionally and a water molecule is linked to the resulting cluster ions. Since the subsequent evolution of the cluster ion occurs in the almost collision free environment of a gas at low pressure, the only passway to relax the excess energy is evaporative cooling rather than collisions. The evaporation efficiency is certainly more rapid if the internal energy of the cluster ion is larger, *i.e.* if the cluster is in its most stable configuration. In that case, the weakest bonds will break for the evaporative cooling to proceed. Since second shell ligands are less strongly bonded to the metal ion than first shell ones, they are thus likely to evaporate. As expected, by Armentrout and coworkers, the ligand exchange source is thus likely to generate the most stable cluster ions, *i.e.* $(Fe, Co)(H_2O)_2^+$ clusters with the 2 water molecules directly attached to the metal, thus stabilizing several isomers of the $M(H_2O)_2^+$ cluster ions.

Smalley type source

In the present Smalley type source, the $M(H_2O)_n^+$ cluster ions are formed during a supersonic expansion. Except when formed by a three body collision, they are initially hot and need to be cooled down for being stabilized. The essential difference with the ligand exchange source is the cooling mechanism: owing to the high gas density at the early stage of the supersonic expansion, collisional cooling by helium is more likely to proceed than radiative cooling. Assuming a collision cross-section of 10 $Å^2$, the typical time between two successive collisions is 10 ns at 300 K when the helium pressure is 1 bar. If the cluster is not too small, this time is short enough to allow cooling before the evaporation of one water molecule. This has been checked for the $Co(H_2O)_2^+$ cluster in an RRKM calculation. It was shown that the filament structure of this cluster is stable for the time between two collisions even if its internal energy is as large as 0.13 eV.

The following picture can then be drawn. During the 10 ns between collisions, the hot clusters have a very floppy structure corresponding to the exploration of the whole phase space accessible to the system in a micro-canonical statistics. A stabilizing collision with helium certainly proceeds in a very short time, less than 2 ps, hence sudden stabilization is expected with no annealing. As a result, the stabilized cluster ion does not correspond necessarily to the thermodynamically most stable one (*i.e.* a trapping in the absolute minimum of the potential energy surface describing the system). Instead, a single collision can stabilize the ion in a high lying well.

References

1. T.F. Magnera, D.E. David, J. Michl, J. Am. Chem. Soc. **111**, 4100 (1989).
2. P.J. Marinelli, R.R. Squires, J. Am. Chem. Soc. **111**, 4101 (1989).
3. R.H. Schultz, P.B. Armentrout, J. Phys. Chem. **97**, 596 (1993).
4. N.F. Dalleska, K. Honma, L.S. Sunderlin, P.B. Armentrout, J. Am. Chem. Soc. **116**, 3519 (1994).
5. M. Rosi, C.W. Bauschlicher Jr, J. Chem. Phys. **90**, 7264 (1989).
6. M. Rosi, C.W. Bauschlicher Jr, J. Chem. Phys. **92**, 1876 (1990).
7. C.W. Bauschlicher Jr, S.R. Langhoff, H. Partridge, J. Chem. Phys. **94**, 2068 (1991).
8. A. Ricca, C.W. Bauschlicher Jr, J. Phys. Chem. **99**, 9003 (1995).
9. A. Fiedler, J. Hrusak, H. Schwartz, Z. Phys. Chem. **175**, 15 (1992).
10. K. Fuke, K. Hashimoto, S. Iwata, Adv. Chem. Phys. **110**, 431 (1999).
11. H. Watanabe, S. Iwata, J. Chem. Phys. **108**, 10078 (1998).
12. H. Watanabe, S. Iwata, J. Phys. Chem. A **101**, 487 (1997).
13. C.S. Yeh, K.F. Willey, D.L. Robbins, M.A. Duncan, Int. J. Mass Spectrom. Ion Proc. **131**, 307 (1994).
14. C.J. Weinheimer, J.M. Lisy, J. Chem. Phys. **105**, 2938 (1996).
15. J. Hrušák, D. Schröder, H. Schwarz, Chem. Phys. Lett. **225**, 416 (1994).
16. D. Feller, E.D. Glendening, W.A. de Jong, J. Chem. Phys. **110**, 1475 (1999).
17. D. Schröder, J. Hrušák, R.H. Hertwig, W. Koch, P. Schwerdtfeger, H. Schwarz, Organometallics **14**, 312 (1995).
18. D. Schröder, H. Schwarz, J. Hrušák, P. Pyykkö, Inorg. Chem. **37**, 624 (1998).
19. O. Sublemontier, L. Poisson, P. Pradel, J.-M. Mestdagh, J.-P. Visticot, J. Am. Soc. Mass Spectrom. **11**, 160 (2000).
20. P. Maître (to be published).
21. T. Baer, W.L. Hase, *Unimolecular Reaction Dynamics* (Oxford, New-York, 1996).
22. G.Z. Whitten, B.S. Rabinovitch, J. Chem. Phys. **41**, 1883 (1964).
23. G.Z. Whitten, B.S. Rabinovitch, J. Chem. Phys. **38**, 2466 (1963).
24. B.H. Mahan, J. Chem. Phys. **52**, 5221 (1970).
25. R.D. Levine, R.B. Bernstein, *Molecular Reaction Dynamics and Chemical Reactivity* (Oxford, New-York, 1987).
26. E. Uggerud, P.J. Derrick, J. Phys. Chem. **95**, 1430 (1991).
27. P. de Sainte Claire, W.L. Hase, J. Phys. Chem. **100**, 8190 (1996).
28. N. Aristov, P.B. Armentrout, J. Phys. Chem. **90**, 5135 (1986).